Fiber Optical Micro-detectors for Oxygen Sensing in Power Plants

Quarterly Technical Report
April 1, 2006 to June 30, 2006

Gregory L. Baker*, Ruby N. Ghosh[+], D.J. Osborn III*, Po Zhang[+]

July 2006

DOE Award Number: DE-FC26-02NT41582

*536 Chemistry Building, Department of Chemistry
[+]2167 BPS, Dept. of Physics

Michigan State University

ABSTRACT

A reflection mode fiber optic oxygen sensor that can operate at high temperatures for power plant applications is being developed. The sensor is based on the $^3O_2$ quenching of the red emission from hexanuclear molybdenum chloride clusters. Our approach towards immobilizing the potassium salt of the molybdenum cluster, $K_2Mo_6Cl_{14}$, at the far end of an optical fiber is to embed the cluster in a thermally cured sol-gel matrix particle. This particle-in-binder approach affords fibers with greatly improved mechanical properties, as compared to previous approaches. The sensor was characterized in 2 - 21 % gas phase oxygen at 40, 70 and 100 °C. These are promising results for a high temperature fiber optical oxygen sensor based on molybdenum chloride clusters.

TABLE OF CONTENTS

LIST OF GRAPHICAL MATERIALS **Page**

INTRODUCTION

Maximizing the efficiency of the combustion process requires real-time control of the correct fuel/oxygen ratio. This requires the ability to sense oxygen levels over a broad range of concentrations with fast response times. Mussell, Newsham, and Ruud previously reported preliminary studies of the synthesis and optical properties of Mo_6Cl_{12}-based clusters relevant to this project [1-4]. Mussell described the synthesis of the molybdenum clusters, and Newsham gives a good account of the properties of neutral Mo_6Cl_{12} clusters and their salts, in both solution and a sol gel matrix. Newsham's data indicate that the photophysical properties of the clusters are maintained in sol gel matrices. To prepare a fiber optic sensor based on Mo_6Cl_{12}, Ruud dispersed Mo_6Cl_{12} in poly[1-trimethylsilyl-1-propyne] (PTMSP), and used a dipping technique to immobilize the composite at the cleaved end of a silica optical fiber. Ghosh and co-workers [5] demonstrated a fast room temperature fiber optic sensor based on oxygen quenching of the luminescence from the PTMSP/Mo_6Cl_{12} composites. While the PTMSP support is adequate for room temperature applications, is unable to withstand the high temperatures associated with combustion in a power plant. To improve the sensor's high temperature performance, we are replacing PTMSP with a thermally stable sol gel matrix that should be able to withstand the higher temperature requirements of the power plant combustion process. The idea of using a sol gel as the support matrix for high temperature oxygen sensor application is not new. Remillard and coworkers have shown that a sol gel supported copper based oxygen sensor can be used in a combustion process [6]. With these facts in hand, we anticipate promising results from our design.

EXECUTIVE SUMMARY

A requirement of optical sensors based on luminescence quenching is that the lumophore have a strong luminescence that is efficiently quenched by oxygen, and that oxygen has ready access to the lumophore. For a high temperature sensor, these characteristics must hold over the entire temperature range of interest.

Previously we described a particle-in-binder approach to immobilizing the potassium salt of a molybdenum cluster, $K_2Mo_6Cl_{14}$, at the tips of optical fibers. This protocol reduced densification and increased the quenching ratios to ~6×. Compared to previous methods, the particle-in-binder approach also affords fibers with greatly improved mechanical properties.

We have measured the response of the fiber sensor to flowing oxygen stream of varying concentration from 2.11 to 21.1 %. A precision gas divider from Horiba (SGD-710C) was purchased and installed up stream from the gas inlet to the heated quartz sensor test chamber. The divider allows us to mix two gases in the ratio of 1:10, 2:10… 10:10. Using a component gas stream of 21.1% O_2 and pure (99.999%) N_2, we are able to generate a flowing gas stream at the following concentrations: (i) 0.001 % O_2, (ii) 2.11 % O_2, (iii) 4.22 % O_2, (iv) 6.32 % O_2, (v) 8.44 % O_2, (vi) 10.6 % O_2, (vii) 12.7 % O_2, (viii) 14.8 % O_2, (ix) 16.9 % O_2, (x) 19.0 % O_2 and (xi) 21.1 % O_2. The precision of the mixed gas is better than 0.5 % of the component gas stream. We are planning future tests of the sensitivity of our sensor to lower oxygen concentrations using primary gas streams of 2% O_2, 0.2% O_2 and 500 ppm O_2.

An extended series of measurements were made on the oxygen sensitivity of a fiber sensor (Fiber sensor 121) up to 100 °C. The sensor tip contains $K_2Mo_6Cl_{14}$ sol-gel particles embedded in an OtMOS / TEOS binder, with roughly 8 x 10^{18} clusters/cm^3, after accounting for the volume contraction in forming the monolith and drying of the particle/binder composite. The data at 42, 73 and 102 °C are in good agreement with theory. We obtain a linear fit of the normalized sensor intensity in 2.1 - 21% gas phase oxygen, to the Stern-Volmer equation. The uncertainty in the slope is only ± 5 %. This slope provides a measure of the sensitivity of our device in detecting gaseous oxygen and is 800, 280 and 160 $[O_2]^{-1}$ at 42, 73 and 102 °C respectively. Although the sensitivity is decreasing with temperature, our sensor can clearly operate up to 100 °C. Considering the linearity of the fit even up to high temperature, we are somewhat puzzled by the fact that the y-intercept does not equal one, within our error bars, as predicted by the Stern-Volmer equation. We are in the process of ruling out any systematic experimental errors.

Other research groups developing oxygen sensing films using a luminescent indicator in a sol-gel matrix have attributed the downwards curvature in the Stern-Volmer plot near zero concentration that we observe to multiple quenching sites in the matrix. In order to determine if such a model is physically significant for our sensing films we need to directly measure the quenching lifetime of Mo-cluster/ sol-gel composite at elevated temperature. As we do not currently have such measurement capabilities at MSU we are looking at an outside vendor for these services.

EXPERIMENTAL

Materials.

All glassware was oven-dried prior to use. Acetonitrile (Spectrum Chemical Company, HPLC grade) was dried over CaH_2 and distilled prior to use. Tetraethyl orthosilicate (TEOS) (Aldrich, 98%), trimethoxy(octyl)silane (OtMOS) (Aldrich, 96%), and hydrochloric acid (CCI, electronics grade) were used as received. Fibers were purchased from Ceramoptec (PUV 1000/1300B), and were handled with gloves in order to minimize surface contamination. Volumes were measured to +/- 0.05 mL.

Cluster-containing Powders for Composites.

mp series, 25-250 μm particles.

Sol-gel solutions containing $K_2Mo_6Cl_{14}$ were aged for 4 – 7 months at room temperature to achieve solid monoliths. The monoliths were then ground using a mortar and pestle and cured at 70 ºC for 5 days to complete the sol-gel reaction and stabilize the particle against further densification. Three series of cluster containing sol-gel powders were prepared; mp31 with a $K_2Mo_6Cl_{14}$ concentration of 8.6×10^{-3} M (cluster source MM5), mp29 with a $K_2Mo_6Cl_{14}$ concentration of 2.1×10^{-3} M (cluster source FJ17), and mp34g-o with a $K_2Mo_6Cl_{14}$ concentration of 2.3×10^{-3} M (cluster source FJ17).

wlb series, 1–8 μm particles.

To obtain smaller particles than are available from grinding using a mortar and pestle, samples from the mp series were pulverized for 15 minutes using a small stainless steel ball mill (Wig-L-Bug).

Sol-Gel Stock Solutions.

TEOS based binder.

The preparation of a typical TEOS-based sol-gel binder solution is described below. TEOS (100 mL, 0.477 mol) and acetonitrile (70.3 mL) were added to a 500 mL Erlenmeyer flask. With stirring, water (32.3 mL, adjusted to pH=1 with HCl) was added and the solution was stirred for 1 hour at room temperature. The stir bar was removed from the flask and the solution was heated in an oil bath at 70 ºC for 2.5 hours. The solution was then transferred to a 500 mL glass bottle, capped, and aged at room temperature until used.

Fiber Coating.

Approximately 1 cm of jacket and cladding were mechanically removed to expose the fiber core. The exposed core was wiped with an acetone-soaked Kimwipe to remove residual cladding material and the tip was suspended in stirred acetone for 30 minutes. The fiber was removed, wiped with an acetone-soaked Kimwipe, rinsed with deionized water, and the fiber tip was suspended in a stirred solution of 2M KOH for 60 minutes. The fibers were removed from the KOH solution, rinsed with 5 mL of deionized water, and then the fiber tips were soaked in deionized water for 30 minutes with stirring. The fibers were removed, rinsed with 5 mL of deionized water, dried using a stream of nitrogen gas, and placed into an oven at 70 ºC for at least 30 minutes.

Scotch tape was used to assemble a flat bundle of five fibers. The ~0.5mm thick fiber jackets ensure that the fiber tips are separated by 1 mm. The bundle of five fibers was dipped by hand at a 15º angle (for better coating of tip) into binder/particle mixtures, being careful to maintain the gap between the fiber tips. The fibers were hung vertically (tip-down) and dried under ambient conditions for one hour to promote uniform coating of the fiber tips.

Optical microscopy of thin films.

Optical microscopy images were acquired using a Nikon Optiphot2-Pol equipped with a Sony Hyper HAD CCD-IRIS/RGB color video camera (model DXC-151A). The camera was connected to a PC using a Sony camera adapter (model CMA-D2). The images were captured using Hauppage computer works Win/TV software (version 2.4.17052).

Fiber optic oxygen sensor characterization system

The response of Fiber sensor 121 to step changes in oxygen from 2 to 21 % O_2, at 40, 70 and 100 °C was measured in the flow through system shown in Fig. 2. This setup has been described in the previously, we summarize its salient features below. Major improvement we have made to the system is to install a Horiba gas divider (SGD-710C) upstream of the gas inlet into the quartz chamber for precise (± %) control over the oxygen concentration. The gas divider allows us to deliver a precise, within ± 0.5% of the component gas (0.1% O_2) stream to the sensor.

Our automated high temperature reflection-mode fiber optic sensor characterization set-up uses a special-design quartz "furnace" to heat the tip of the fiber sensor up to ~110 °C and monitor the temperature to better than ± 2 °C using a thermocouple placed 1 – 2 mm near sensor tips. The gas flows in this flow- through cell is 400-300 mL/min. By monitoring both the inlet (±10 sccm) and outlet (±20 sccm) flows, we estimate a gas exchange time 10s for the system. We use a Labview program to simultaneously monitor the sensor signal and sensor temperature. The excitation source for the sensor measurements is about 700 μW, at the wavelength of 365 nm UV Nichia LED. Using the dichroic beam splitter and the UV objective lens we are able to couple around 300 μW into the multimode fiber (Φ 1mm core diameter) by a UV objective lens. The reflected phosphorescence (590 – 850 nm) from the tip of the fiber sensor is collected by the photomultiplier tube (PMT). A 45 ° dichroic beam splitter and a 590 nm long wave pass (LWP) filter are used to separate the pump and signal beams. The detection optics/electronics consists of a Hamamatsu Detector R955 and a Stanford SR570 current pre-amplifier. The typical gain of the preamplifier used is 20 μA/V. We estimate that a 1 V signal at the voltmeter corresponds to 1 nW of phosphorescence signal from the fiber sensor. In addition we estimate that the "unwanted" light in the emission bandwidth that reaches the detector to a level 1/160 of the smallest sensor signal in oxygen

The entire optical path from the UV LED to the detector is aligned on a *single* optical bench plate, which has the following advantages. First we are able to make meaningful long term, over several days, sensor measurements because of the stability of both the pump power coupled in the fiber sensor as well as the coupling of the output sensor

signal to the detector. Secondly, we are able to remove a fiber sensor from the measurement system and reinstall it with a high degree of reproducibility (repeatability of LED to fiber coupling of better than 1%), which allows for meaningful comparisons between one sensor and another.

Gas Divider - SGD 710C

In the experiment, we need to accurately determine the oxygen concentration of the flowing gas stream. The Horiba gas divider (SGD -710C) was used to mix 21.1% oxygen (component gas) with 99.999% N_2 (dilution gas) as shown in Fig 1. The precision of the gas divider is 0.5 % of the component gas, i.e. 0.1 % O_2 in our case, with a repeatability of 0.2 % of the component gas. The gas divider consists of 10 identical capillary tubes. A mechanical switch sets the number of capillaries used for the component and dilution gas, such that the generated gas of concentration C, is given by $C = m/10\ C_o$, where C_o is the concentration of component gas (oxygen), and m is the number of capillaries in which component gas flows. The inlet pressure of the capillary tubes is controlled by a pressure regulating section which is precisely designed to allow the pressure of a component gas (O_2) to remain same as that of a N_2 gas (dilution). The generated flow rate then depends upon only on the pressure of the dilution gas which we selected 5 psi. The generated flow has usually 10psi pressure.

To make measurement between two preset oxygen levels, we replace the gas divider with a 3–way solenoid valve (Cole-Parmer Inc. EW-98302-42) to automatically switch between the two gases. The time duration of each gas pulse can be set by the switch controller. This system allows us to perform long-term gas cycling measurements with flow rate from 100 to 1000 sccm/

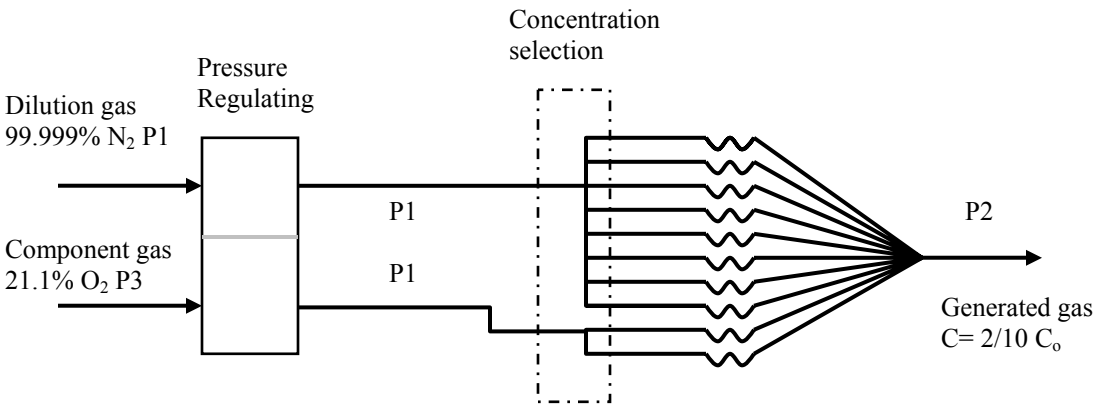

Figure 1. Schematic of gas divider SGD-710 principle

Molar oxygen concentration [O_2]

To calculate the molar oxygen concentration in the flow through cell at a given temperature T and pressure *p* we use the ideal gas law:

$$pV = nRT,$$

hence, molar oxygen concentration $[O_2] = n/V = p/(TR)$

Where n is the number of moles of the gas, R = 8.2057 x 10^{-2} l atm/mol/K is universal gas constant. T is absolute temperature in K,
The measured pressure *p* in our flow through cell is 10 psi or 0.6803 atm. For a given oxygen fraction F (where F =1 for 100%) the molar oxygen concentration is

$$[O_2] = n/V = 8.29F/T$$

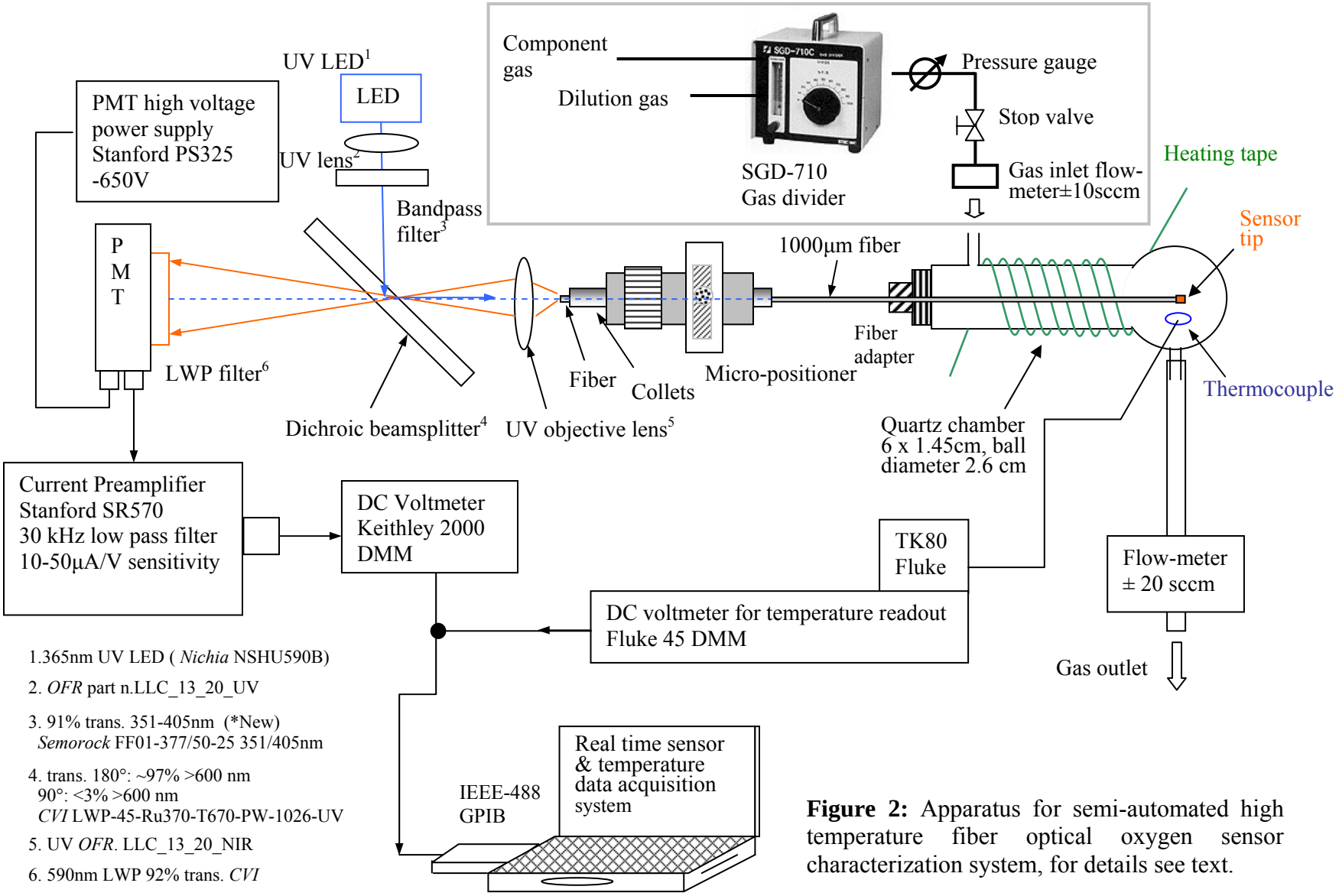

Figure 2: Apparatus for semi-automated high temperature fiber optical oxygen sensor characterization system, for details see text.

RESULTS AND DISCUSSION

Composite Approach to Sol-gel Matrices Containing $K_2Mo_6Cl_{14}$ Clusters on Fiber Substrates.

Our recent emphasis has been to immobilize molybdenum clusters at the end of high-temperature optical fibers using methods that ensure high luminescence intensity from the clusters and strong quenching of the luminescence in the presence of oxygen. Previously we discovered that despite long aging and drying times, films deposited on substrates continued to evolve when they were tested at high temperatures. In general the quenching ratio decreased, which is consistent with densification of the sol-gel matrix. Our hypothesis is that in these materials, the limiting factor in the quenching process is the diffusion of oxygen to the molybdenum clusters, and that the oxygen diffusivity in the heat-treated sol-gel matrices was low. Both the change in the physical parameters of the sol-gel matrix and the low quenching ratio are problems that must be solved in any practical sensor.

As outlined previously, we developed a composite material approach that involves embedding molybdenum-containing sol-gel particles in a binder that essentially glues the particles to the substrate (**Figure 4**). This approach offers several advantages that will overcome some of the limitations encountered when depositing a homogeneous solution of the cluster in a sol-gel solution. First, by using a preformed and fully equilibrated cluster-containing sol-gel matrix, issues related to the long-term aging of the sol-gel matrix are avoided. Second, the use of small particle sizes should lead to large quenching ratios, since for small particles the diffusivity of oxygen should be dominated by the permeability of the binder. We expected that the binder, a minority component of the matrix, would fill the void space between the small particles and provide good particle-particle adhesion, and that the curing process would lead to little if any net change in the volume of the composite.

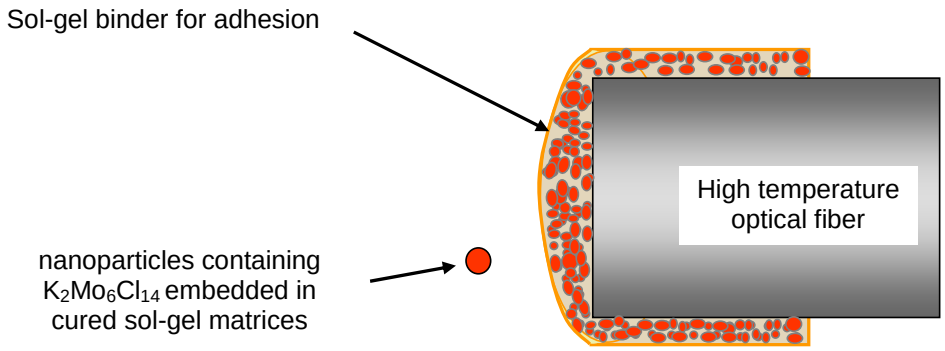

Figure 3. Schematic showing the expected morphology resulting from dip or spray coating a slurry of particles in a sol-gel binder solution. The particles correspond to pre-cured sol-gel particles containing $K_2Mo_6Cl_{14}$ clusters.

Multifiber Dip-coating of Fiber Sensors

We moved from single fiber dipping to dip-coating a 5-fiber array to minimize fiber-to-fiber variation **(Figure 4)**. In principle, this process can be scaled to allow simultaneous coating of a large number of fibers. Access to fibers with similar properties enables parallel testing of fibers under a broad range of conditions. Different cluster/sol-gel monoliths were tested to optimize sensor performance and adhesion for each case. The smaller particles obtained using a small ball mill gave better adhesion and sensor performance.

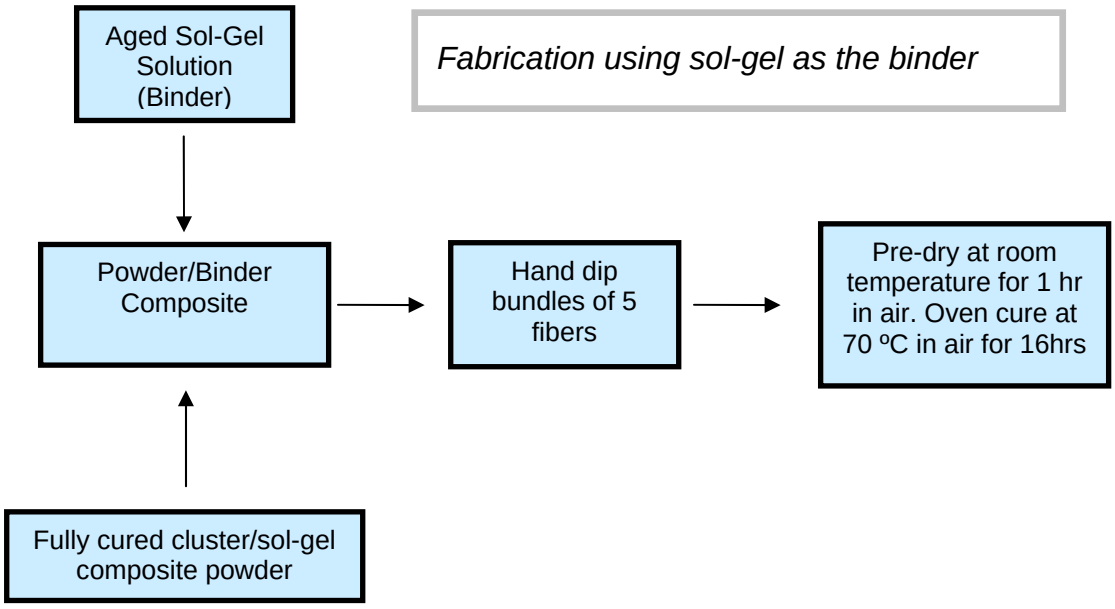

Figure 4. Processing schemes used for coating fiber bundles.

Oxygen Sensitivity of Fiber Sensors at Elevated Temperatures

An extended series of measurements were made on the oxygen sensitivity of the fiber sensor up to 100 °C. All the data are from Fiber sensor 121, see Fig. 5 for photographs of the as fabricated sensor and after all thermal testing. The sensor tip contains $K_2Mo_6Cl_{14}$ sol-gel particles embedded in a OtMOS / TEOS binder matrix. The sensing film was cured for 16 hours at 70°C. The tip contains roughly 8 x 10^{18} clusters/cm^3, after accounting for the volume contraction in forming the monolith and drying of the particle/binder composite.

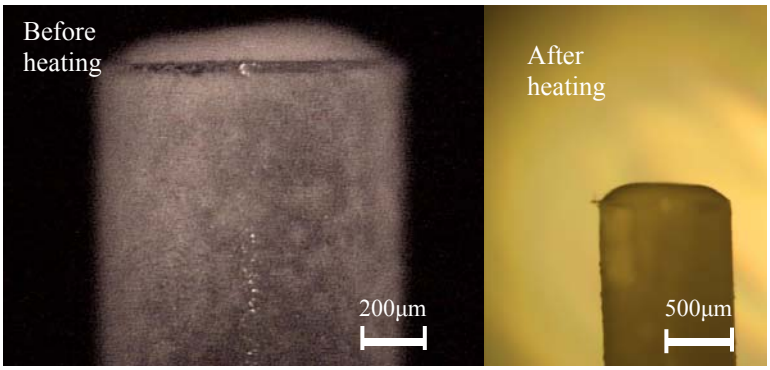

Figure 5. Photograph of Fiber 121 as fabricated and after all thermal testing

Fiber Sensor 121 at 42 °C

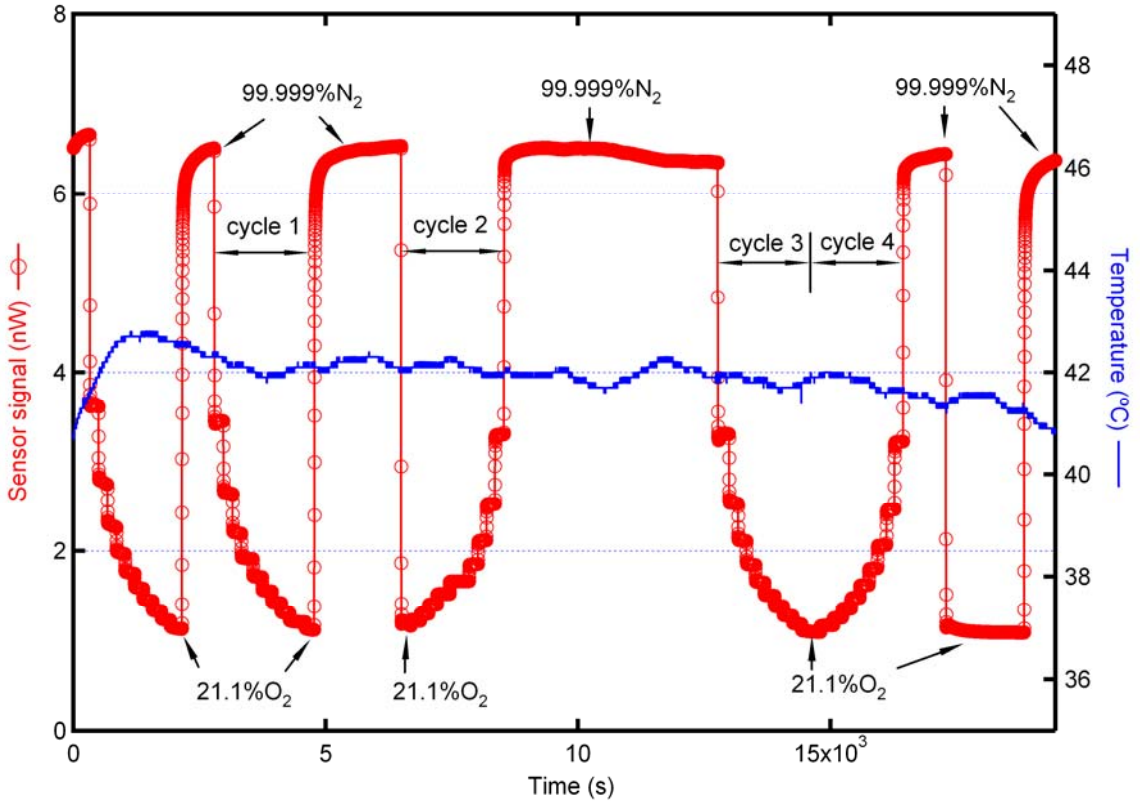

Figure 6. Oxygen sensitivity of Fiber 121 at 42 °C during several cycles of measurement. The gas composition for each cycle was: (i) 99.999 % N_2, (ii) 2.11 % O_2, (iii) 4.22 % O_2, (iv) 6.32 % O_2, (v) 8.44 % O_2, (vi) 10.6 % O_2, (vii) 12.7 % O_2, (viii) 14.8 % O_2, (ix) 16.9 % O_2, (x) 19.0 % O_2 and (xi) 21.1 % O_2, with the balance N_2. Note during the two cycles from 6,500 – 10,000 s and 14,580 – 17,062 s the gas order was reversed going from 21.1 % O_2 to 99.999 % N_2. Coupled pump power is 285 μW, gas flow rate is 400 and 370 sccm at the input and output of the quartz chamber respectively, and the cluster concentration is ~8 x 10^{18} clusters/cm^3 .

The oxygen response of Fiber sensor 121 over several cycles from 2 to 21% O_2 at 42 °C are shown in Fig. 6. The device is easily able to detect changes in oxygen concentration at the percent level at this temperature. The data was taken in our flow through system, with the sensor exposed to each gas concentration for about 3 minutes. The wait time in pure nitrogen was significantly longer to allow the device to equilibrate. The temperature stability of our system is quite good, over the 5.5 hours the temperature held at 41.9 ± 0.4 °C.

The quenching of cluster luminescence by oxygen is expected to obey the Stern-Volmer relationship [7,5]

$$I_0/I = 1 + k_q \tau_0 [O_2]$$

Where I_0 and I are the luminescence intensities in the absence and presence of oxygen of concentration $[O_2]$ and k_q is the quenching rate constant and τ_0 the luminescence lifetime in the absence of oxygen. The inverse of the luminescence intensity at a given oxygen concentration normalized with respect to the unquenched intensity, I_0/I is plotted in Fig. 7. Each measurement point in Fig. 7 is the average value of the normalized sensor signal from cycle 1 – 4 of Fig. 6. The fit is to the Stern-Volmer relationship is quite good. We obtain a linear relationship between I_0/I and $[O_2]$, with a slope of 800 $[O_2]^{-1}$ and an intercept of 1.5. The uncertainty in the slope is only ± 5%.

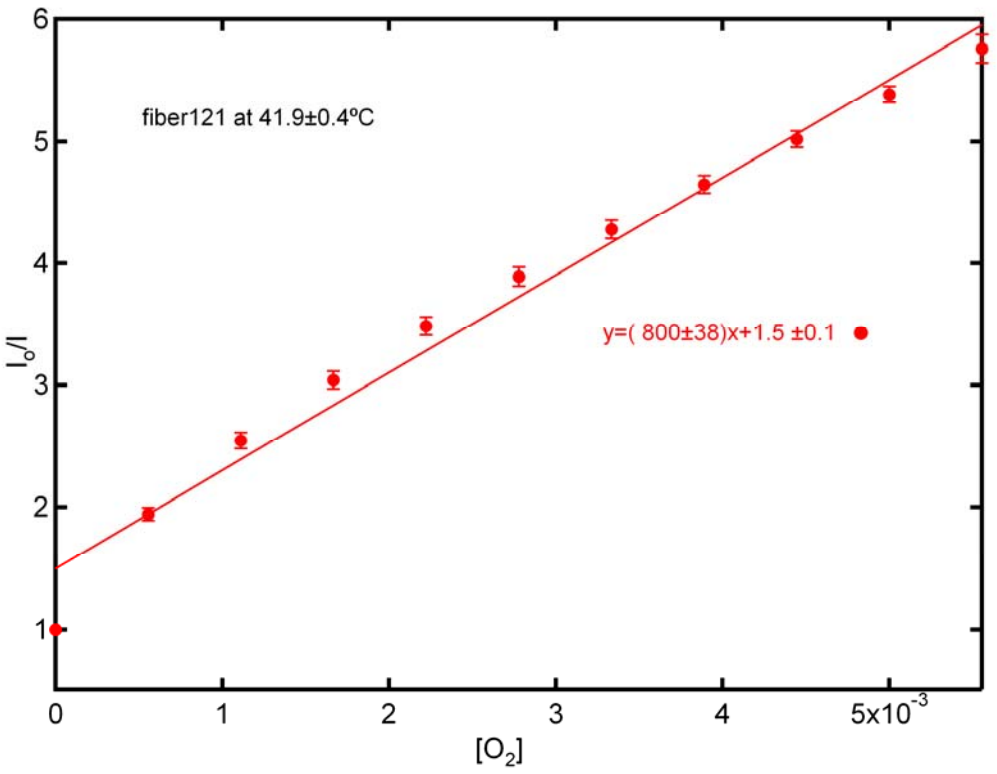

Figure 7. Stern-Volmer relationship, I_0/I as a function of molar oxygen concentration, at 42 °C for Fiber sensor 121. The data are from Fig. 6 and represent the average over the indicated four cycles.

Fiber Sensor 121 at 73 °C

Shown in Fig. 8 is the oxygen response of the sensor at 73 °C. The Stern-Volmer plot was obtained by averaging the measurements from four complete cycles between pure nitrogen and 21 % oxygen. We again obtained a good linear fit between I_0/I as a function of $[O_2]$, with a slope of 280 $[O_2]^{-1}$ ± 5 % and an intercept of 1.16.

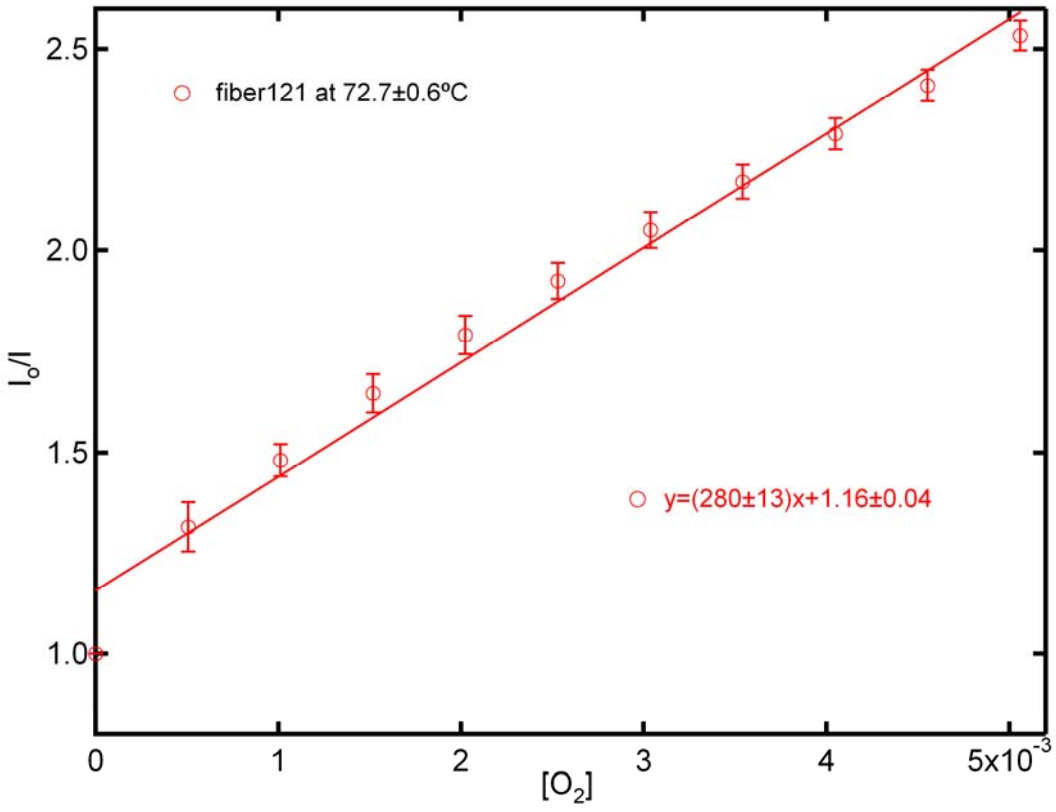

Figure 8. Stern-Volmer relationship, I_0/I as a function of molar oxygen concentration, at 73 °C for Fiber sensor 121. Plotted is the average from four cycles of measurement. Coupled pump power is 285 μW, gas flow rate is 400 and 390 sccm at the input and output of the quartz chamber respectively.

Fiber Sensor 121 at 102 °C

Shown in Fig. 9 is the oxygen response of the sensor at 102 °C. The Stern-Volmer plot was obtained by averaging the measurements from two complete cycles between pure nitrogen and 21 % oxygen. Even at this elevated temperature, we have a good linear fit between I_0/I as a function of $[O_2]$, with a slope of 160 $[O_2]^{-1}$ ± 4 % and an intercept of 1.07.

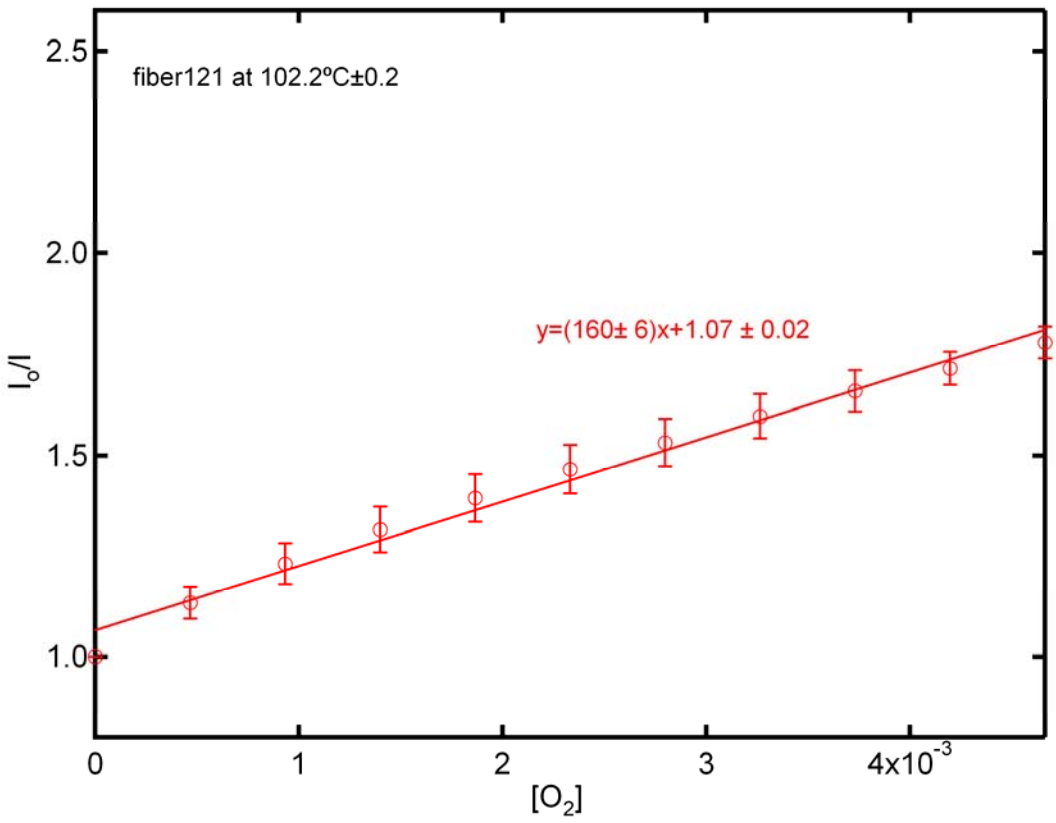

Figure 9. Stern-Volmer relationship, I_0/I as a function of molar oxygen concentration, at 102 °C for Fiber sensor 121. Plotted is the average from two cycles of measurements. Coupled pump power is 285 µW, gas flow rate is 400 and 370 sccm at the input and output of the quartz chamber respectively.

Sensor temperature °C	Sensor Sensitivity $[O_2]^{-1}$
42	800 ± 5%
73	280 ± 5%
102	160 ± 4%

Table 1. Slope of the linear Stern-Volmer plot, "sensor sensitivity" at elevated temperatures, from the data is Fig. 7, 8 and 9.

The slope of the linear Stern-Volmer plot provides a measure of the sensitivity of our device towards detection of gaseous oxygen. As shown in Table 1, although the sensitivity is decreasing with temperature our sensor is able to operate up to 100 °C. Considering the linearity of the fit even up to high temperature, we are somewhat puzzled by the fact that the y-intercept does not equal one, within our error bars, as predicted by the Stern-Volmer equation. We need to further analyze of our data to rule out the following experimental problem, i.e. that there is a systematic error in our calculation of the molar oxygen concentration.

Room temperature oxygen sensing experiments by other research groups [8], using a luminescent indicator in a sol-gel matrix, also report a downwards curvature in the Stern-Volmer plot near zero concentration as we observe. A phenomenological multiple site model has been invoked to fit such data. However, at present the structural evidence in support of multiple types of quenching sites in the sol-gel matrix is rather weak. In addition the quenching lifetimes obtained from fitting the data in the Stern-Volmer plot to a multi-site model, is in poor agreement with the directly measured luminescence lifetimes. We will need to directly measure the quenching lifetime of our molybdenum cluster/ sol-gel composite sensing film to resolve this question. Unfortunately, we do not currently have access to system that would allow us to determine the lifetime of our material at elevated temperature.

CONCLUSIONS

We are encouraged by the oxygen sensitivity results from our fiber sensor operating between 42 and 102 °C. The fit to the linear Stern-Volmer equation is good, with a slope of 160 $[O_2]^{-1}$ at the highest temperature. However, the reason for the y-intercept not equally one within the uncertainty of the fit is still under investigation. The composite approach of using $K_2Mo_6Cl_{14}$ / sol-gel particles immobilized in an OtMOS/TEOS binder matrix gives us fiber sensors with the required mechanical stability to withstand high temperature. In the next period we will need to repeat the lower temperature measurements, i.e. 40 °C, after the higher temperature excursions, to ascertain whether the performance of the device remains stable higher temperature excursions. Our concern is that in the past we have observed continual evolution o f the sol-gel matrix with time and temperature cycling which results in changes in oxygen diffusivity in the matrix. We are investigating whether curing the sensors at 70 °C under vacuum will "age" the sensor quickly resulting in a more stable sensing behavior for long term measurements.

REFERENCES

[1] R. D. Mussell, Ph. D. thesis, Michigan State University (East Lansing), **1988**.

[2] M. D. Newsham, Michigan State University (East Lansing), **1988**.

[3] M. D. Newsham, M. K. Cerreta, K. A. Berglund, D. G. Nocera, *Mater. Res. Soc. Symp. Proc.* **1988**, *121*, 627.

[4] C. J. Ruud, Ph. D. thesis, Michigan State University (East Lansing), **1999**.

[5] R. N. Ghosh, G. L. Baker, C. Ruud, D. G. Nocera, *Appl. Phys. Lett.* **1999**, *75*, 2885.

[6] J. T. Remillard, J. R. Jones, B. D. Poindexter, C. K. Narula, W. H. Weber, *Appl. Opt.* **1999**, *38*, 5306

[7] Otto S. Wolfbeis (ed), Fiber optic chemical sensor and biosensors, vol I, CRC press 1991, p. 84-87.

[8] Y. Tang, E. C. Tehan, Z.Tao, and F.V. Bright, *Anal. Chem.* **2003,** *75, pp2407-2413*.

BIBLIOGRAPHY

None.

LIST OF ACRONYMS AND ABBREVIATIONS

HCl – Hydrochloric Acid
MeOH – Methanol; CH_3CN – Acetonitrile
TEOS – Tetraethyl orthosilicate
OtMOS – trimethoxy(octyl)silane
OtEOS – octyltriethoxysilane
TFP-tMOS – trimethoxysilane;
PtMOS – propyltrimethoxysilane

APPENDIX A - ACKNOWLEDGEMENTS

We wish to acknowledge the contribution of Reza Loloee, Michigan State University, towards the gas flow switch box and design of new gas flow through cell and Per Askeland, Michigan State University, regarding discussion on the thermal properties of various sol-gel binders. The Labview program for sensor data acquisition was developed by Mr. Nate Verhanovitz (Troy Research Systems, LLC)